Journal of Chemical&Engineering Data

pubs.acs.org/jced Article

MOFX-DB: An Online Database of Computational Adsorption Data for Nanoporous Materials

N. Scott Bobbitt, Kaihang Shi, Benjamin J. Bucior, Haoyuan Chen, Nathaniel Tracy-Amoroso, Zhao Li, Yangzesheng Sun, Julia H. Merlin, J. Ilja Siepmann, Daniel W. Siderius, and Randall Q. Snurr*

Cite This: https://doi.org/10.1021/acs.jced.2c00583 Read Online

ACCESS | Metrics & More | Article Recommendations | Supporting Information

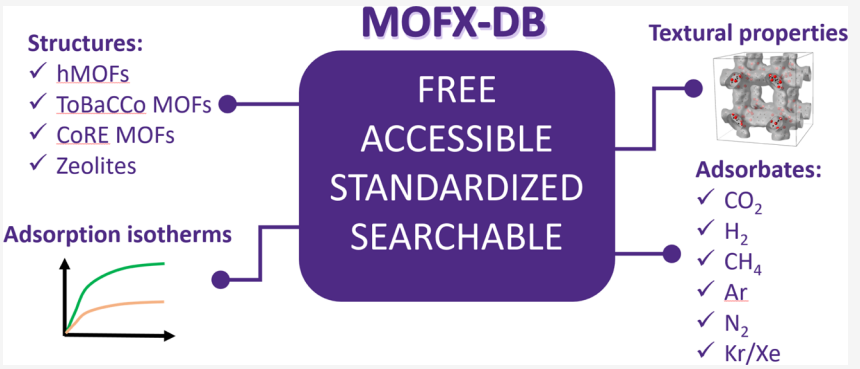

ABSTRACT: Machine learning and data mining coupled with molecular modeling have become powerful tools for materials discovery. Metal−organic frameworks (MOFs) are a rich area for this due to their modular construction and numerous applications. Here, we make data from several previous large-scale studies in MOFs and zeolites from our groups (and new data for N_2 and Ar adsorption in MOFs) easily accessible in one place. The database includes over three million simulated adsorption data points for H_2, CH_4, CO_2, Xe, Kr, Ar, and N_2 in over 160 000 MOFs and 286 zeolites, textural properties like pore sizes and surface areas, and the structure file for each material. We include metadata about the Monte Carlo simulations to enable reproducibility. The database is searchable by MOF properties, and the data are stored in a standardized JavaScript Object Notation format that is interoperable with the NIST adsorption database. We also identify several MOFs that meet high performance targets for multiple applications, such as high storage capacity for both hydrogen and methane or high CO_2 capacity plus good Xe/Kr selectivity. By providing this data publicly, we hope to facilitate machine learning studies on these materials, leading to new insights on adsorption in MOFs and zeolites.

1. INTRODUCTION

Metal−organic frameworks (MOFs) are porous crystals made of inorganic nodes connected by organic linkers.[1] MOFs can be constructed from many different types of nodes and linkers, including various functional groups, and the building blocks can be arranged in a wide variety of topological networks. The modular nature of MOF construction and the vast assortment of available building blocks and topologies result in a combinatorial explosion in the number of possible unique MOF structures. To date, over 14 000 unique MOFs have been synthesized representing more than 350 topologies,[2] and hundreds of thousands more have been predicted computationally.[3−7] The number of possible MOF structures is likely well into the millions or even billions.

Owing to the vast chemical space represented by MOFs, many research groups have turned to computational high-throughput screening and machine learning to find candidates well-suited to specific applications.[8−11] Computational screening has been used to identify promising MOFs for applications including gas storage,[6,12,13] separations,[14−17] carbon capture,[18,19] refrigeration,[20−22] catalysis,[23,24] and chemical sensing.[25,26]

These large-scale computational studies have generated an enormous amount of data for the adsorption behavior of different adsorbates in a huge number of MOFs. Some groups have successfully mined this data after it was originally published, leading to new and deeper insights. For example, Fernandez *et al.*[27] analyzed previous methane adsorption data from Wilmer *et al.*[3] to develop quantitative structure−property relationships that can accurately predict methane adsorption

Received: September 13, 2022
Accepted: December 19, 2022

solely from easy-to-compute geometric properties of MOFs. Ahmed *et al.* assembled about half a million MOFs from various online databases and analyzed them for hydrogen storage, resulting in the synthesis of three MOFs that have storage capacity exceeding the previous record-holder IRMOF-20.[28] Bucior *et al.* used previous data from Bobbitt *et al.*[29] to train a machine learning model that can accurately and rapidly predict hydrogen storage capacity in MOFs.[30] Iacomi and Llewellyn[31] used a high-throughput methodology to process 32 000 adsorption isotherms from the NIST Database of Novel and Emerging Adsorbent Materials[32] (NIST-ISODB) and predict materials with potential binary separation capabilities. Published databases of structures can also be used to generate data for new applications. For example, the original CoRE MOF database published by Chung *et al.* in 2014 contains about 4700 experimental MOF structures that have been organized and made ready for computational studies.[33] This paper and an update from 2019[2] have been cited over 750 times, which is a testament to the usefulness of online databases. Similarly, the MOF subset of the Cambridge Structural Database, published by Moghadam *et al.*, has been cited over 650 times since 2017.[34] By reanalyzing previously published data to gain new insight or repurposing data to a new application, these studies maximize the value of the initial effort (both computation and human effort) required to generate this data.

While data accessibility clearly has value, in reality, most data are only available in scattered and disparate forms, if at all. The data published in journal articles is often selectively reported to include only the most relevant portions for a paper, while the full set of data might not be published. The data that is available are not provided in any standard format, typically a spreadsheet or PDF file posted in the Supporting Information of a journal article. These nonstandard formats are not amenable to automated data collection and require significant manual effort to organize into a form that can be combined with data from other groups. Furthermore, the details of how these data were generated might be incomplete, which is a challenge for reproducibility. Graduate students and postdocs who did much of the work eventually move on to other jobs, and the original files and institutional knowledge are lost.

A study on data availability by Vines *et al.* found that the probability of a data set being available fell 17% per year with the age of the article, and the probability of finding a valid email address for the corresponding author fell by 7% per year.[35] Some groups say they will make specific data available upon request; however, in practice, this method is also unreliable. Authors may move or retire or simply be too busy to respond to requests for data. Krawczyk and Reuben performed a social experiment by requesting data related to economics research from 200 groups *via* email.[36] They received responses from only 64% of the subjects, and even fewer (44%) actually sent the data. Another recent study by Gabelica *et al.* found even more dire results: of the 1792 authors who were contacted with requests for data, less than 7% (122 authors) actually provided the data.[37] This highlights the need for data to be made publicly available.

Many groups have realized this problem and made efforts to improve the situation. Some have published extensive data sets online with their published articles.[3,18,38] This is a valuable step, but isolated sets of data are still of limited utility. Researchers who might want the data must first know where to find it, and the data might not be in an easily retrievable or accessible format. Also, data that is tied to specific journal articles might be hidden behind subscriptions or paywalls that are not accessible to the general public. There remains a need for more standardized and open databases of materials data. A recent survey by the American Chemical Society published in a Chemical & Engineering News white paper reports that over half of the nearly 700 respondents said that lack of standardization between data formats was the biggest pain point in their data management plan.[39]

Coudert[40] recently called for open, standardized databases for materials using a set of guidelines called "FAIR," which is an acronym for **F**indable, **A**ccessible, **I**nteroperable, and **R**eusable.[41] These guidelines require that data be

1. Findable: data should be easily found, indexed, and searchable
2. Accessible: data are retrievable using a standard protocol that is open and free
3. Interoperable: data are organized in a well-defined format with metadata included
4. Reusable: data contains all relevant metadata needed to reuse or reproduce it

Here we present MOFX-DB (mof.tech.northwestern.edu), a new database of computational data for adsorption in MOFs based on numerous previous studies carried out by the Snurr group and other members of the Nanoporous Materials Genome Center. MOFX-DB meets all the FAIR guidelines described above: it is easily searchable, freely accessible, and all the data and metadata are available for download in a self-describing, computer-readable format.

MOFX-DB contains computational data for seven different adsorbates in over 160 000 MOFs and in 286 zeolites. It includes textural properties for each structure (*e.g.*, surface area and pore size) as well as metadata, such as force field parameters and simulation details. Users can quickly search the database using a built-in graphical user interface (GUI) to find MOFs with specific properties or data for particular adsorbates of interest. All of the data and structure files can be downloaded in a convenient format. Each data point is also linked to a digital object identifier (DOI) for the original paper (if previously published) so that the origin of all the data are documented.

We also present here a standardized format for archiving isotherm adsorption data based on the JavaScript Object Notation (JSON) format used in the NIST-ISODB, which has been extended here to include simulation details such as number of Monte Carlo cycles and information about the force field. This format can be used for both single-component and multi-component isotherms. We encourage the nanoporous materials community to consider this format as a standard for reporting isotherm data.

We offer this data to the public in the hope that it will facilitate new data mining or machine learning studies that lead to greater understanding of adsorption in MOFs and possibly the discovery of useful materials for applications that have not yet been considered. In this paper, we describe in detail the format and functionality of MOFX-DB to empower other research groups to access the data for their own projects and adopt the JSON format for reporting their own data.

We also simulated nitrogen (at 77 K) and argon (at 87 K) isotherms for all of the CoRE MOFs and added these results into MOFX-DB. Comparison of computational and experimental N_2 and Ar isotherms is a common characterization

https://doi.org/10.1021/acs.jced.2c00583
J. Chem. Eng. Data XXXX, XXX, XXX−XXX

Table 1. Summary of Data Included in MOFX-DB with Original References[a]

database	adsorbate(s)	*P*, bar	*T*, K	references
CoRE MOF	Ar	0−1	87	this work
CoRE MOF	N_2	0−1	77	this work
hMOF	CO_2	0.01, 0.05, 0.1, 0.5, 2.5	298	Wilmer *et al.*[42]
hMOF	H_2	2, 100	77	Bobbitt *et al.*[29]
ToBaCCo	H_2	6, 100	77	Gómez-Gualdrón *et al.*[43]
ToBaCCo	H_2	5	160	Gómez-Gualdrón *et al.*[43]
ToBaCCo	H_2	100	130, 200, 243	Colón *et al.*[4]
IZA	H_2	1, 2.71, 7.39, 20.09, 30, 54.6, 148.4, 403.4	77, 92.4, 110.88, 133.06, 159.67, 191.6, 229.92, 275.9	Sun *et al.*[46]
PCOD-syn	H_2	1, 2.71, 7.39, 20.09, 30, 54.6, 148.4, 403.4	77, 92.4, 110.88, 133.06, 159.67, 191.6, 229.92, 275.9	Sun *et al.*[46]
hMOF	CH_4	35	298	Wilmer *et al.*[3]
hMOF	CH_4	0.05, 0.5, 0.9, 2.5, 4.5	298	Wilmer *et al.*[42]
ToBaCCo	CH_4	6, 65, 100	298	Colón *et al.*[4]
hMOF	N_2	0.09, 0.9	298	Wilmer *et al.*[42]
hMOF	Xe/Kr (0.2/0.8)	1, 5, 10	273	Sikora *et al.*[16]
ToBaCCo	Xe/Kr (0.2/0.8)	1, 5	298	Colón *et al.*[4]

[a]CoRE MOF, hMOF, and ToBaCCo databases are for MOFs, and IZA and PCOD-syn databases are for zeolite structures.

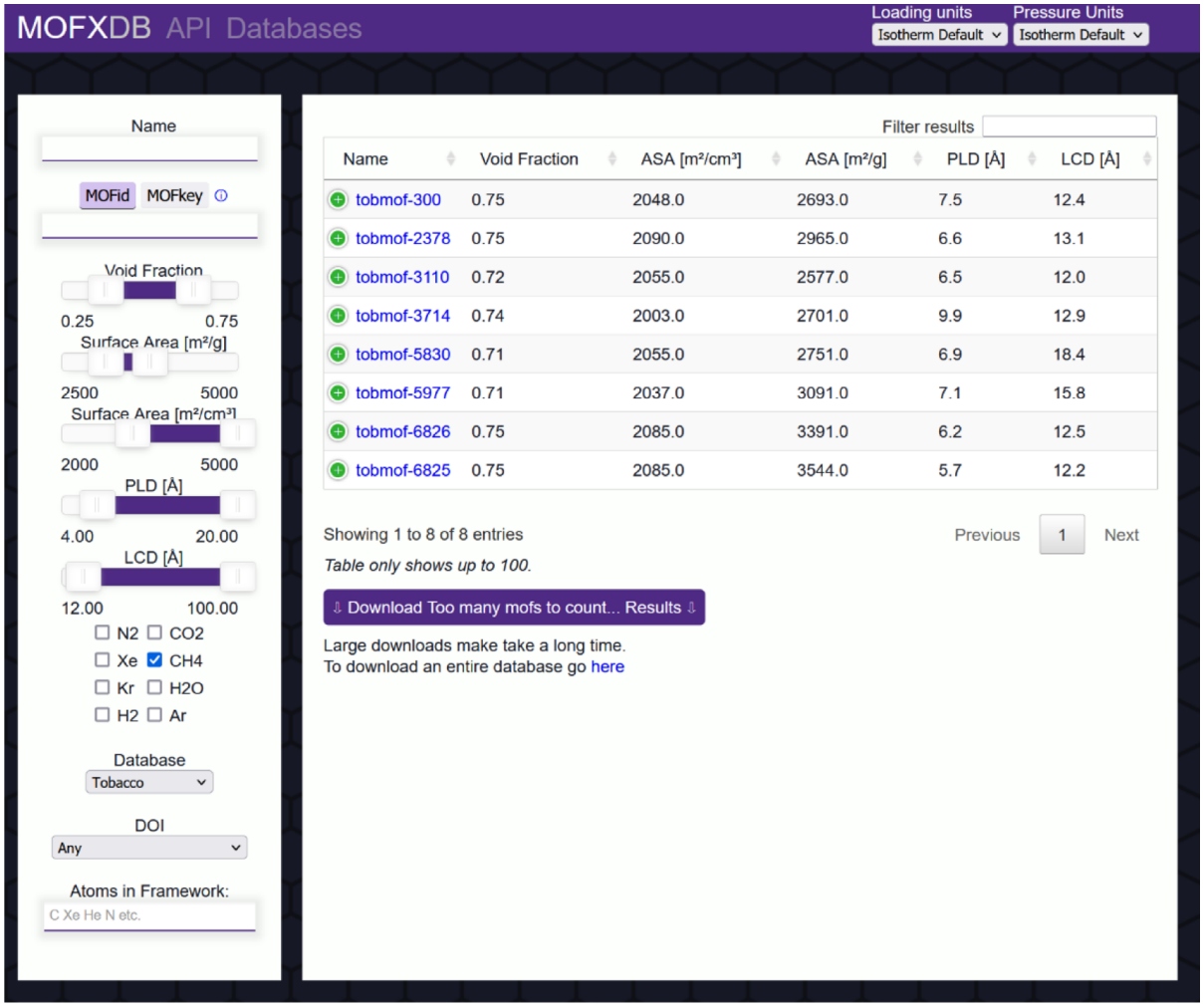

Figure 1. Screenshot of search results for methane adsorption data and specified geometric properties. The search criteria can be easily modified with the slider bars on the left of the screen. More information about each MOF can be seen by clicking on the MOF name.

technique to determine if a MOF is fully activated or has experienced pore collapse. By comparing experimental isotherms to the nitrogen and argon isotherms we publish here, synthesis groups can have confidence that MOFs they have made in the lab are well-activated and have surface areas that are close to the maximum expected value for a perfect crystal.

Finally, as an example of the useful, novel analysis enabled by this database, we present a study of MOFs that hit high performance targets for multiple applications simultaneously,

https://doi.org/10.1021/acs.jced.2c00583
J. Chem. Eng. Data XXXX, XXX, XXX−XXX

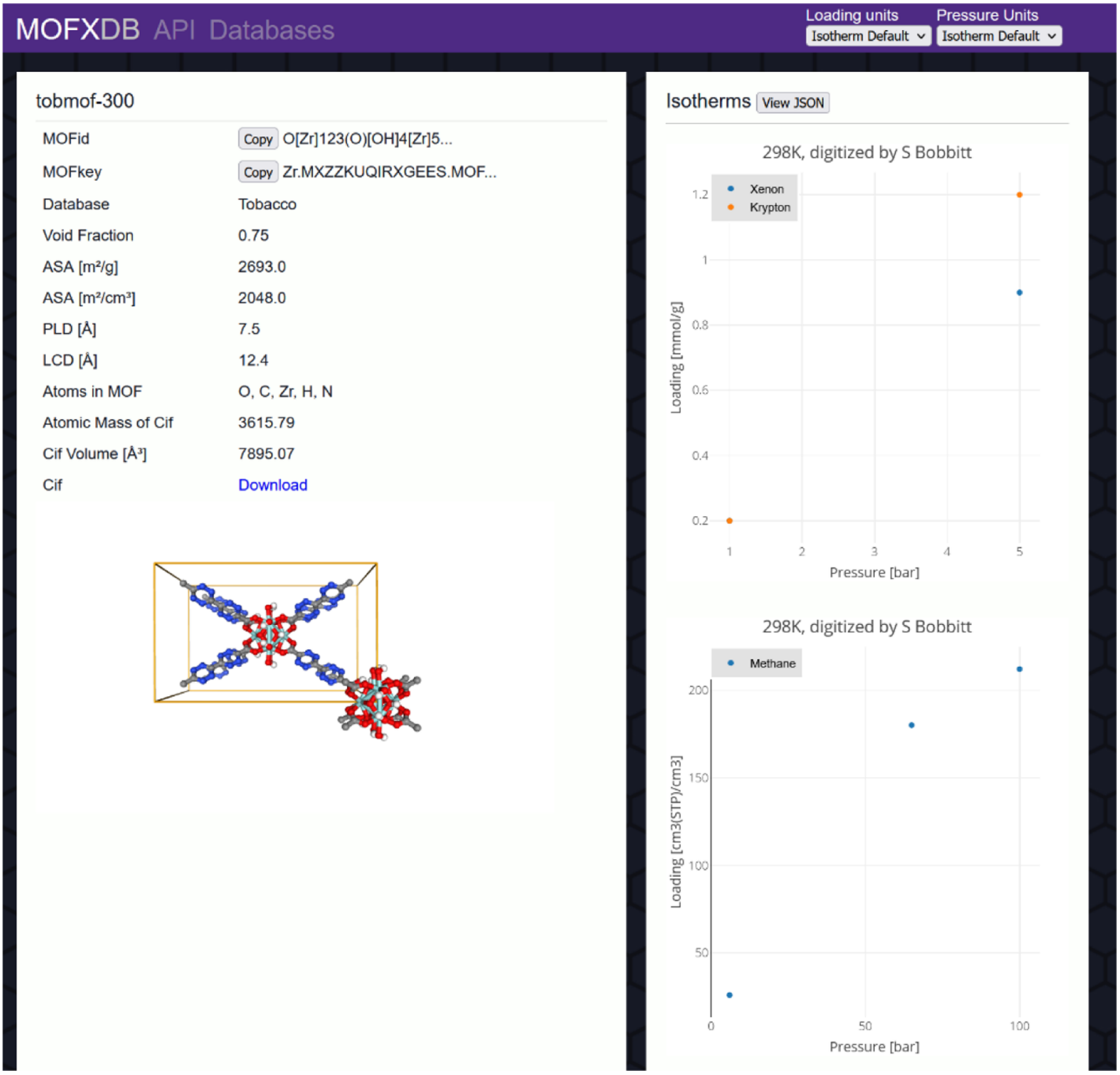

Figure 2. Screenshot of database page for the MOF tobmof-300 from the search results described in Figure 1. The page includes textural properties, a visualization of the crystal structure, and adsorption data. The simulation details and isotherm data can be accessed by clicking "View JSON" in the upper right.

which we believe might lead to greater commercial interest in MOF-based technology.

2. CONTENT AND USAGE OF MOFX-DB

2.1. Contents of MOFX-DB. MOFX-DB contains computed adsorption data for over 160 000 MOFs, both real and hypothetical, based on the work from the Snurr group at Northwestern University and collaborators.[3,4,16,29,33,42,43] The specific adsorbates, MOF and zeolite structure databases, and corresponding references are summarized in Table 1. The hMOF[3] and ToBaCCo[4] structure databases were constructed by geometrically assembling MOF building blocks *in silico*. We note that originally 13 512 ToBaCCo MOFs were reported, including a null structure with no atoms. Here we exclude this null structure, and a total of 13 511 valid ToBaCCo MOFs are reported in MOFX-DB. The CoRE MOF database[2,33] contains MOF crystal structures originally derived from experiment with additional post-processing steps to become computation-ready. We included both the 2014[33] version and the 2019[2] version in MOFX-DB. For CoRE MOF 2014, a total of 4764 structures were available.[44] For CoRE MOF 2019, a total of 12 020 all-solvent-removed (ASR_public) structures were taken from the original paper, which now corresponds to version 1.1.0 in the Zenodo repository.[45]

For each of the isotherm points summarized in Table 1, the database provides all of the essential information needed to reproduce the simulation, including temperature, pressure, force field parameters, structure file (CIF), and Monte Carlo simulation details such as the number of cycles used. Details of the simulations are also given in Table S5. Most entries also

https://doi.org/10.1021/acs.jced.2c00583
J. Chem. Eng. Data XXXX, XXX, XXX−XXX

include the original input file for the simulation software RASPA,[47] if it was available. Each entry also contains a DOI reference that links to the original published paper.

To demonstrate the expandability of the database, we also uploaded 2288 published adsorption isotherms (a total of 18 304 data points) for simulated hydrogen capacity in zeolites[46] to the MOFX-DB with a wide range of temperature and pressure conditions. The zeolite structures include 216 all-silica zeolites taken from the International Zeolite Association (referred to as "IZA" in MOFX-DB) and 70 hypothetical all-silica zeolites with high predicted synthesizability (Predicted Crystallography Open Database, referred to as "PCOD-syn" in MOFX-DB). Due to the standardized format of the JSON files used in the database, adding data from other groups is convenient and fast. Data can be arranged into a formatted comma-separated values (CSV) file and uploaded with database tools we developed (see Supporting Information Section S1).

2.2. Using MOFX-DB. The database can be accessed at mof.tech.northwestern.edu. The frontpage contains a GUI that can be used to search the database for materials with certain properties. The database contains many features to enable users to easily find the information they want. Users can search for data using the common or systematic (MOFid and MOFkey[48]) names of MOFs, ranges of textural properties, or specific atoms contained in the MOF (*e.g.*, MOFs that contain the element Cl). Users can also search for MOFs that have adsorption data for specific adsorbates. Figure 1 shows an example of a search for data on methane adsorption in MOFs from the ToBaCCo database with void fractions ranging from 0.25 to 0.75, gravimetric surface areas ranging from 2500 to 5000 m^2/g, volumetric surface areas ranging from 2000 to 5000 m^2/cm^3, with pore-limiting diameters (PLDs) above 4.0 Å and largest cavity diameters (LCDs) above 12.0 Å. The desired limits for properties like void fraction, surface area, and pore size can easily be input using the slider bars on the left of the screen. The search finds 8 MOFs that fit these criteria, which are summarized in the table on the right of the screen. More information about each MOF can be accessed by clicking the MOF name. Users also have the option to download a zip file with all the CIFs of these MOFs or an Excel sheet, PDF file, or CSV file with the adsorption and textural data.

Note that the web page shows only 100 matches at a time, but if there are more results, they can all be downloaded in a zip file. Users who want all of the data for a specific database can also download those files from the "Databases" tab.

The webpage for each specific MOF shows a summary of textural properties (void fraction, surface area, PLD and LCD) that are associated with the original paper where the corresponding adsorption isotherms were reported, as well as a rotatable visualization of the MOF crystal structure. All the available adsorption data (including adsorption isotherms and heats of adsorption) for that MOF are also displayed. We note that because textural properties were collected from different publications published over a period of several years by various authors, they were calculated with inconsistent parameters, procedures, and programs. To ensure a fair comparison of MOFs across the entire MOFX-DB, we re-calculated textural properties (referred to as "consistent set") for all MOF structures using a set of consistent guidelines. We made this "consistent set" a separate data set, and they can be downloaded from the "Databases" tab on the MOFX-DB website under the name "Download Textural Properties." See Supporting Information Section S2 for more details. The textural properties reported on zeolite pages were calculated using the same consistent rules detailed in Section S2.2 (because the textural properties are unavailable in the original paper) but with a different set of adsorbent force field parameters designed for zeolites.[46] Clicking on a specific MOF or zeolite name on the front page search results brings up a more detailed page for that material. Figure 2 shows a screenshot of the landing page for tobmof-300, which was selected from the search results described in our previous example, along with adsorption data for methane (single-component) and Xe/Kr (mixture) in this MOF. Each page also contains the unique MOFid and MOFkey identifiers,[48] which are useful for cheminformatics and data mining.

Users can access more details about the simulation by clicking on the "View JSON" button on the upper right. The JSON file contains the CIF file for the MOF, all the adsorption data, searchable InChIKeys[49] for the adsorbates, and information about the simulation and force field. Each entry also contains a DOI link to the original paper.

These JSON files are compatible with the NIST-ISODB adsorption database but are also expanded to include simulation metadata. The structure of the JSON file is discussed in further detail in Section 3.2. Additionally, the isotherm JSON files can be obtained through a representational state transfer (REST) application programming interface (API) to facilitate further analysis, as described in Section 2.3.

The ability to search for MOFs based on properties can be used to find new MOFs that match textural properties that others have previously determined to be desirable for an application. The MOF literature is full of high-throughput studies in which researchers analyze the pore size, pore shape, surface area, and void fraction that offer the best performance for a given gas storage or separation application.[8,50] Here, we examine one such study on Xe/Kr separation and apply the design principles they suggested to find other MOFs in our database that also have outstanding Xe/Kr performance.

Banerjee *et al.* screened over 125 000 MOFs from the literature (including the hMOFs and CoRE MOFs included in this database) for high Xe/Kr selectivity using simulated and experimental Henry constants.[51] They concluded that the MOF SBMOF-1[52] (KAXQIL in the CSD) had the best performance due to its ideal LCD of 5.1 Å. In fact, many of the MOFs in their study with LCDs near this size showed high Xe selectivity over Kr. However, they observed that their chosen MOF, SBMOF-1, has relatively low Xe capacity compared to other MOFs due to its low gravimetric surface area (145 m^2/g). The measured capacity of Xe in SBMOF-1 at 298 K and 1 bar is 1.38 mmol/g. Therefore, we hypothesized that if we could identify additional MOFs with a similar pore size and higher surface area, they would likely have similarly high selectivity and better Xe capacity. The databases screened by Banerjee *et al.* included the hMOFs and CoRE MOFs, which are in our database, but they did not include the ToBaCCo MOFs, so we started our search there.

Using the interface on the website, we searched for all MOFs from the ToBaCCo database that have LCD between 4.8 and 5.4 Å and surface areas greater than 200 m^2/g. The kinetic diameter of Xe is 3.96 Å, so we also limited our search to MOFs with a PLD greater than 4.0 Å to permit diffusion of Xe into the pores. This search resulted in eight MOFs that fit these criteria, and from these eight MOFs, there are four with Xe capacity equal to or above 2.0 mol/kg for a 20/80 gas-phase

https://doi.org/10.1021/acs.jced.2c00583
J. Chem. Eng. Data XXXX, XXX, XXX−XXX

Table 2. Textural Properties and Xe/Kr Adsorption Data for 4 MOFs from the ToBaCCo Database That Fit the Prescribed Properties from Banerjee *et al.*[51a]

name	void fraction	SA (m^2/g)	PLD (Å)	LCD (Å)	Xe (mol/kg)	Kr (mol/kg)	selectivity
SBMOF-1	0.25[b]	145[b]	4.2[b]	5.1[b]	1.2 (0.2 bar)[c]	0.9 (0.8 bar)[c]	16[c]
SBMOF-1 (sim)	0.25[b]	120[d]	3.9[d]	4.5[d]	1.45[e]	1.43[e]	
tobmof-4188	0.47	230	4.0	5.0	3.9	1.0	15.6
tobmof-4906	0.46	353	4.7	5.3	2.5	0.8	12.5
tobmof-4199	0.44	266	4.2	5.2	2.4	1.0	9.6
tobmof-4905	0.48	247	4.2	5.0	2.0	0.8	10.0

[a]Adsorption properties for ToBaCCo MOFs are computed for a 20/80 Xe/Kr mixture at 1 bar and 298 K. Sorted by Xe capacity. [b]Surface area, PLD, and LCD for SBMOF-1 are taken from Banerjee *et al.* Void fraction for SBMOF-1 was computed for this work using He insertions in RASPA. [c]Adsorption and selectivity values for SBMOF-1 are taken from experimental single component isotherms (Banerjee *et al.*). [d]Surface area, PLD, and LCD were computed in Zeo++ using a probe radius of 1.86 Å and high accuracy flag. [e]Simulated in RASPA using single component at 298 K and 0.2 bar for Xe and 0.8 bar for Kr to match the experiments reported by Banerjee *et al.*

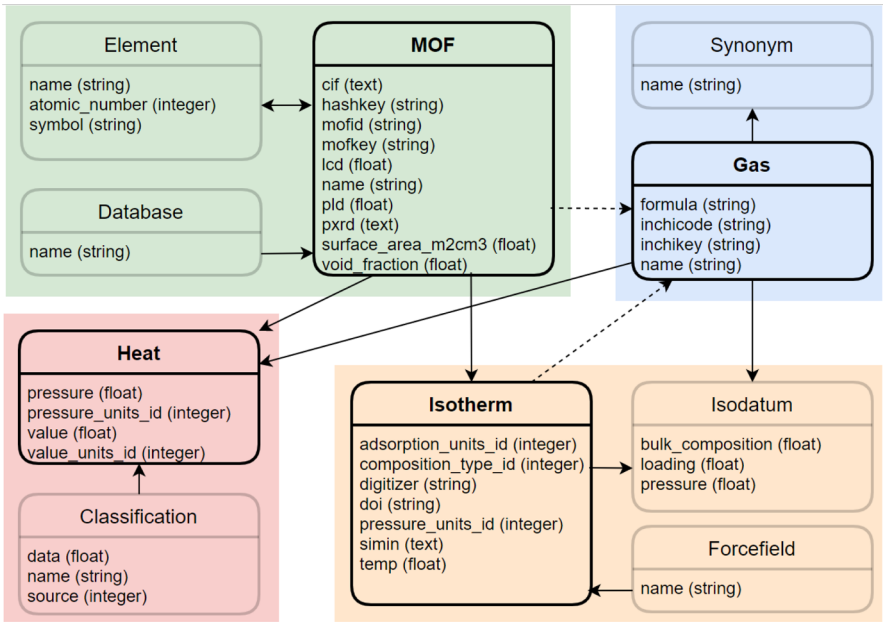

Figure 3. Schematic of the organizational structure of MOFX-DB. The solid lines indicate dependencies between two tables, and the dashed lines indicate associations. The direction of the arrows indicates the directionality of the relationship between two tables (*e.g.*, MOFs have associated isotherms, which consist of isodata). Tables are grouped together and highlighted as a guide to the reader, indicating the key concepts of MOF materials, adsorbates, and simulation data for isotherms and heats of adsorption.

mixture at 1 bar and 298 K, as shown in Table 2. The most promising MOF, tobmof-4188, has a Xe capacity of 3.9 mol/kg with selectivity of 15.6 at these conditions. This is significantly greater than the reported saturation capacity of SBMOF-1, which was about 1.4 mol/kg for pure Xe, and the predicted selectivity is comparable to the measured value of 16 for SBMOF-1.

2.3. Automated Data Retrieval. In addition to the web-based GUI for interacting with the database, users can also run automated queries using an API. We follow the conventions of RESTful web services[53] to allow users to query the database for MOFs matching certain textural properties or to download isotherm data. Per REST API conventions, software can issue the GET verb (as opposed to POST, DELETE, or PUT) to retrieve data from a source. Using GET is supported in many programs such as the curl project, the requests module in Python, or by visiting the URL for the API endpoint in a web browser. For example, to run the same search query from Figure 1, a program could issue a GET request as https://mof.tech.northwestern.edu/mofs.json?database=Tobacco&vf_min=0.25&vf_max=0.75&sa_m2g_min=2500&sa_m2g_max=5000&pld_min=4.0&lcd_min=12.0&gases=Methane to encode all the relevant parameters and receive a filtered list of MOFs. Not all of the search criteria are required: the API will only filter by properties that are specified in the query. For example, to search the ToBaCCo database by surface area, a program could use a query of https://mof.tech.northwestern.edu/mofs.json?database=Tobacco&sa_m2g_min=2500&sa_m2g_max=5000. Data from the databases can also be sorted and downloaded using a requests module in Python 3, such as in the following example.

```
$ pip3 install requests
import requests
resp = requests.request('GET', 'https://mof.tech.northwestern.edu/mofs.json',
        headers={'loading': 'cm3(STP)/cm3', 'pressure': 'bar'},
        params={'vf_min': 0.5, 'vf_max': 1})
resp = resp.json()
print(resp.keys())
>> ['results', 'pages', 'page']
```

A native Python package called "mofdb_client" has also been developed to facilitate the data retrieval from MOFX-DB. Further details are available on the website: https://mof.tech.northwestern.edu/api.

https://doi.org/10.1021/acs.jced.2c00583
J. Chem. Eng. Data XXXX, XXX, XXX−XXX

3. STRUCTURE OF MOFX-DB AND ISOTHERM JSON FILES

3.1. Structure and Design of MOFX-DB. The underlying organizational structure of MOFX-DB is shown in Figure 3, along with the types of information stored in each field. In general, the database tables contain information about the MOFs, their textural properties, adsorbate identification, and adsorption isotherm data including simulation details. We store the relevant tables of data in a MySQL database, which facilitates specification of the relationships between the different types of data and rapid data storage and retrieval using standard relational database tools. Specifically, we are using the Ruby on Rails framework and its conventions for our database schema. Rails uses a "convention over configuration" mantra to facilitate consistent normalized schemas.

The website user interface and API routes are hosted using an application stack consisting of Phusion Passenger for the application server, Ruby on Rails for application and view logic, and MySQL as a database server. The website's backend code is an open source project on GitHub at https://github.com/snurr-group/MOFdb.

3.2. Format of the Isotherm JSON File and Compatibility with NIST. MOFX-DB outputs isotherm data in a format informally known as the "JSON isotherm file." This format for descriptively encoding adsorption isotherm data and metadata was introduced by NIST as part of NIST-ISODB,[54] originally for single-component isotherms and later expanded to describe multicomponent isotherms. For a full description of the JSON isotherm file and its thermodynamic basis, please see the Supporting Information, Section S3; we provide a summary of the JSON isotherm file format here. We note that another isotherm standard file, the "adsorption information file," has been proposed recently,[55] primarily to aid archiving and comparison of isotherms from different adsorption instruments.

The JSON isotherm file represents an isotherm *via* a set of key−value pairs that identify the relevant metadata about an isotherm as well as the adsorption data, while avoiding ambiguity about the meaning of those data and metadata. In short, the isotherm file describes the conditions of the adsorptive phase,[56] the adsorption measurements, and the identity of the adsorbent material and adsorbate species. It is compact, self-describing, and readable by both humans and computers, as the key−value pairs are composed of unencoded text or arrays of key−value pairs. For example, the following text block is an artificial example of a JSON-encoded isotherm that exemplifies the key−value pairs necessary to describe an adsorption isotherm:

```
{
   'temperature': 300,
   'adsorbent': {'name': 'CuBTC'},
   'adsorbates': [{'name': 'CO2'}],
   'isotherm_data': [
      {'pressure': 1.,
       'species_data': [{'name': 'CO2',
                         'adsorption': 2.,
                         'composition': 1.}]
      },
      {'pressure': 3.,
       'species_data': [{'name': 'CO2',
                         'adsorption': 6.,
                         'composition': 1.}]
      }
   ]
   'adsorptionUnits': 'mmol/g',
   'compositionType': 'molefraction',
   'pressureUnits': 'Pa',
}
```

In this format, there is unambiguous identification of the adsorbent, adsorbate, measurement/simulation conditions, and adsorption isotherm data (uptake), such that the isotherm can be reproduced by another research group. (We point out that this is a *minimal* set of key−value pairs for describing an isotherm; other explanatory metadata may be added to the JSON file, such as more specific identifiers for the adsorbent and adsorbate(s), other relevant measurement conditions, *etc.*) In this example, we are showing single-component data, so the mole fraction of CO_2 is reported as 1.

MOFX-DB builds on the JSON isotherm file from NIST-ISODB by introducing additional key−value pairs related to the molecular simulations that are ultimately the source of isotherms herein. Specifically, the MOFX-DB JSON file carries key−value pairs that describe the forcefields for both the adsorbate(s) and adsorbent ("molecule_forcefield" and "adsorbent_forcefield", respectively), references to the exact representation of the adsorbent material structure, and a full writeout of the RASPA input file for the source simulation. Consequently, the isotherm given in the JSON file should be reproducible by another research group based on the metadata stored therein.

The JSON file output by the MOFX-DB API is compatible with that used by NIST-ISODB and can be used interchangeably following straightforward conversions related to adsorbent identification and units of measurement. This use demonstrates the flexibility and adaptability of the JSON format, in that it can be adapted to a use case where isotherm measurements are communicated in a consistent fashion, while carrying metadata specific to the intentions of the particular project. The JSON isotherm format has the potential to be a field-wide, consistent format used by the adsorption community to ensure clarity and consistency in the description of adsorption isotherm measurements, while allowing for group- or project-specific adaptations.

3.3. MOFX-DB Versions. We expect to add more data to the database over time, and it is possible that mistakes will be found and corrected in the published data. Similarly, we expect that, in the future, researchers may perform validation simulations for the same sorbent structure and the same force field, but potentially using longer simulation trajectories or different software that may supplant a previous version of this isotherm. To maintain a record of edits and revisions to MOFX-DB, there is an archival repository on GitHub that automatically collates changes. The current version number of MOFX-DB is shown on the website footer and is included in any JSON files or bulk file downloads. Previous versions can be

https://doi.org/10.1021/acs.jced.2c00583
J. Chem. Eng. Data XXXX, XXX, XXX−XXX

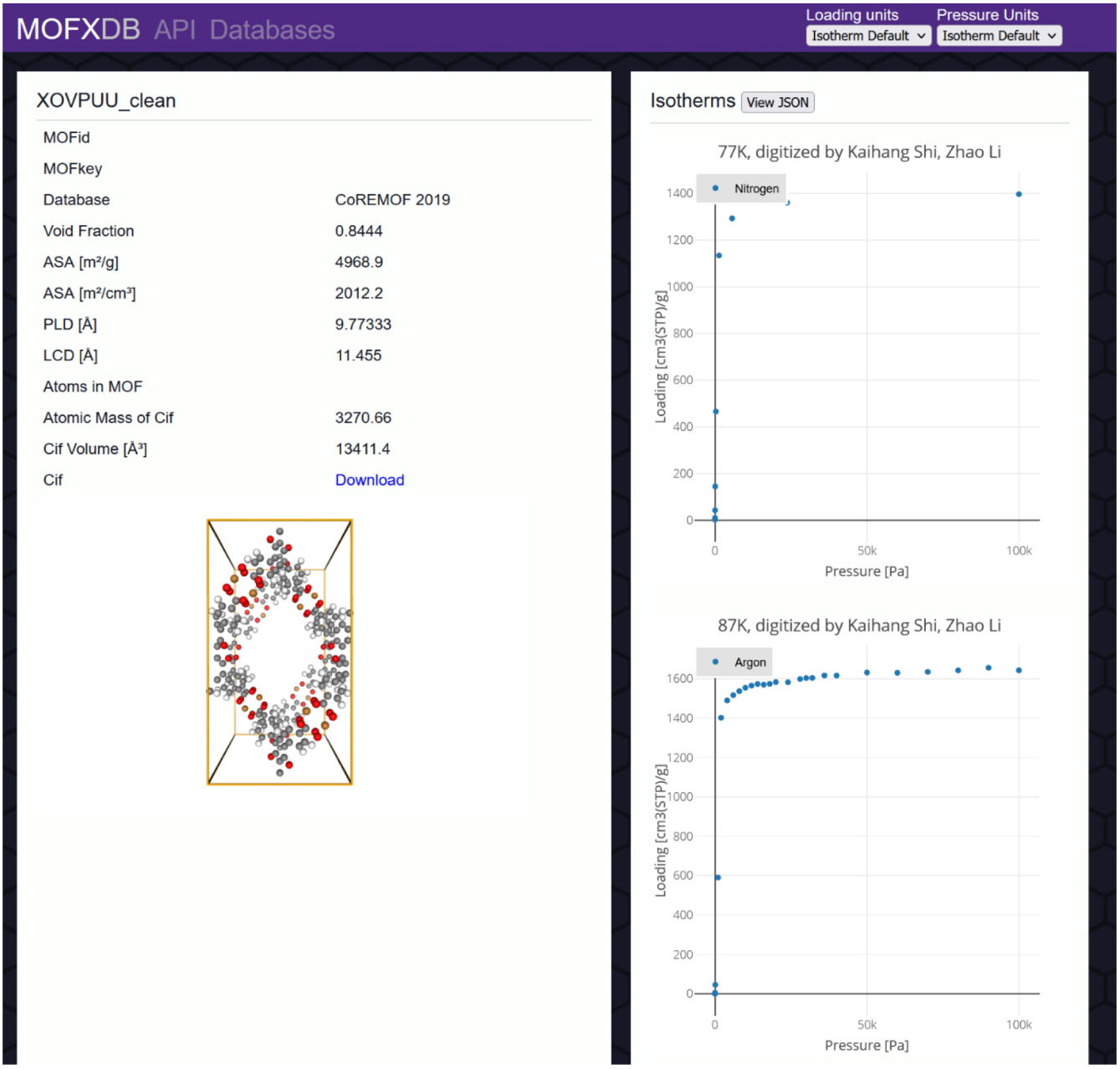

Figure 4. Screenshot of the database page for the MOF with CSF refcode "XOVPUU".

found using the command "git checkout version." We encourage all researchers using MOFX-DB data to include the version of MOFX-DB they used for their work to ensure transparency and reproducibility. More details are given in the Supporting Information.

4. RESULTS

4.1. Comparison of Simulated and Experimental Data. *4.1.1. Nitrogen and Argon Isotherms.* We performed simulations for N_2 (at 77 K) and Ar (at 87 K) to calculate isotherms for all of the CoRE MOFs[2] and included this data in MOFX-DB. Nitrogen and argon isotherms at those temperatures (their boiling points) are commonly used in experiments to characterize MOFs after synthesis. Comparison of experimental isotherms to simulated isotherms for ideal crystals can provide insight into the activation of the MOF (*i.e.,* completeness of solvent removal) and also possibly indicate if the pores have collapsed. Experimental isotherms that agree with simulated isotherms provide a high degree of confidence that the MOF structure corresponds with what is expected. By providing this data, we hope it will be useful to synthesis groups to quickly benchmark their measured results. Unlike some of the data provided in the database, this is new data that has not been previously published elsewhere.

Nitrogen or argon adsorption data for a specific MOF can be accessed from MOFX-DB by typing the name of the desired MOF in the search box. As an example, we searched for "XOVPUU" which is a MOF from the CoRE MOF 2019 database and has relatively high surface area.[57,58] As shown in Figure 4, we were able to directly visualize the nitrogen and argon isotherms in the MOF, both of which exhibited pore filling and saturation loading at the high pressure.

The isotherms were computed using the multipurpose molecular simulation code RASPA.[47] The interatomic

https://doi.org/10.1021/acs.jced.2c00583
J. Chem. Eng. Data XXXX, XXX, XXX−XXX

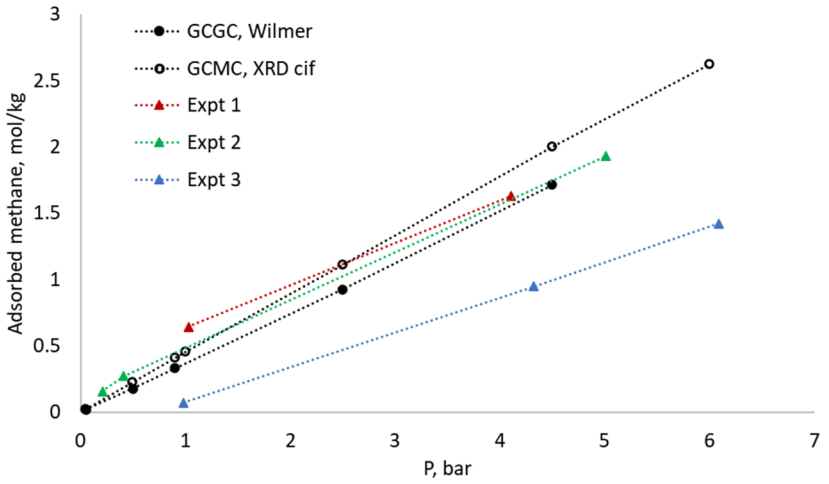

Figure 5. Simulated isotherms overlaid on experimental results taken from the NIST adsorbent data base. Units are converted to mol/kg from the units originally reported. All isotherms are at 298 K. Simulation data in black solid circles were taken from Wilmer *et al.*[42] GCMC data from an XRD structure (block hollow circles) were computed in this work using a structure file from Eddaoudi *et al.*[68] Expt 1 taken from Pillai *et al.*[62] Expt 2 taken from Li *et al.*[63] Expt 3 taken from Furukawa *et al.*[65]

interactions used Lennard-Jones parameters from UFF[59] for the MOF framework atoms and the TraPPE force field[60] for nitrogen. The TraPPE N_2 force field includes Lennard-Jones sites on the nitrogen atoms and three charge sites (−0.482 on the nitrogen atoms and 0.964 on the center of mass). Argon was treated as a single Lennard-Jones sphere using the parameters ε/k_B = 115 K and σ = 3.407 Å.[61] Lennard-Jones interactions between adsorbates and framework atoms beyond a cutoff of 12.8 Å were neglected, and we used a simulation box that was at least twice the cutoff (25.6 Å) in all dimensions. No charges were included on the framework atoms, and the N_2/N_2 electrostatic interactions were treated with the Ewald method. For Ar−Ar interactions, we included tail correction beyond the cutoff radius. Isotherms were computed at pressure points ranging from 0 to 1 bar at 77 K for nitrogen and at 87 K for argon. We used 7500 (15 000) initialization cycles and 7500 (15 000) production cycles for N_2 (Ar), thus 15 000 (30 000) total cycles. A cycle includes N Monte Carlo moves, where N is the number of molecules in the system at the beginning of the cycle, or 20 moves if N is less than 20. Details of simulations are given in Table S5.

4.1.2. Comparison with Experimental Methane Data from NIST. A benefit of having a large set of adsorption data available online is that future researchers can easily check their results against known quantities. In the field of MOF synthesis, incomplete activation or partial pore collapse are common issues that can affect the amount of gas adsorbed in a MOF due to reduced surface area or pore volume. Simulations, of course, give ideal results considering adsorption into a perfect crystal. Therefore, comparing experimental results to simulated data can give researchers insight into whether their MOF is fully activated or perhaps if there were problems during the synthesis or activation.

Figure 5 shows an example of simulated methane data in IRMOF-1 (also called MOF-5 or in this database hMOF-0) at 298 K from Wilmer *et al.*[42] compared with several experiments.[62−65] The experimental data are taken from the NIST adsorption database, which is also compatible with our database. Two of the experimental isotherms agree well with the simulated one, while one has significantly lower methane adsorption. This might be an example of pore collapse or incomplete activation during the synthesis of that MOF. Figure 5 also shows a isotherm from grand canonical Monte Carlo (GCMC) simulations using a structure file derived from X-ray diffraction (XRD) experiments[66,67] (downloaded from the Cambridge Structure Database,[68] CCDC no. 256965), for comparison with the idealized hMOF-0 structure generated *in silico* used in Wilmer's calculations. The difference between these two simulated isotherms highlights the importance of reporting exact structures (*e.g.,* as CIF files in Supporting Information) along with published data. There can be significant differences in simulated or experimental crystal structures that are nominally the same material. Computer-generated structures can also differ if, for example, they are minimized using different force fields or minimization routines. A benefit of MOFX-DB is that users can download a file with the exact structure that was used for a simulation, along with other important metadata to enable reproducibility.

4.2. Usage Example: Searching for MOFs Suitable for Multiple Applications. *4.2.1. Motivation.* While most of the data contained in MOFX-DB has already been thoroughly analyzed for some specific application described in the original papers, the data are also a valuable resource for identifying MOFs that might be suitable for other adsorption applications that might have different performance requirements or figures of merit.

One of the great and oft-cited benefits of MOFs is their tremendous customizability. By choosing the best combination of nodes and linkers, MOFs can be optimized to maximize desired performance metrics for various applications. One alternative to producing bespoke MOFs for each application of interest is to focus on developing MOFs that can meet the requirements of multiple applications. This could potentially reduce the production costs by allowing larger quantities of MOFs to be synthesized at a facility without having to retool the equipment for different products. In short, it might be more economical to manufacture a few MOFs that meet acceptable—if not record-setting—performance targets for several applications instead of one "ideal" MOF for each application.

Here we demonstrate how MOFX-DB can help to identify such MOFs. Instead of finding the single best MOF for a

https://doi.org/10.1021/acs.jced.2c00583
J. Chem. Eng. Data XXXX, XXX, XXX−XXX

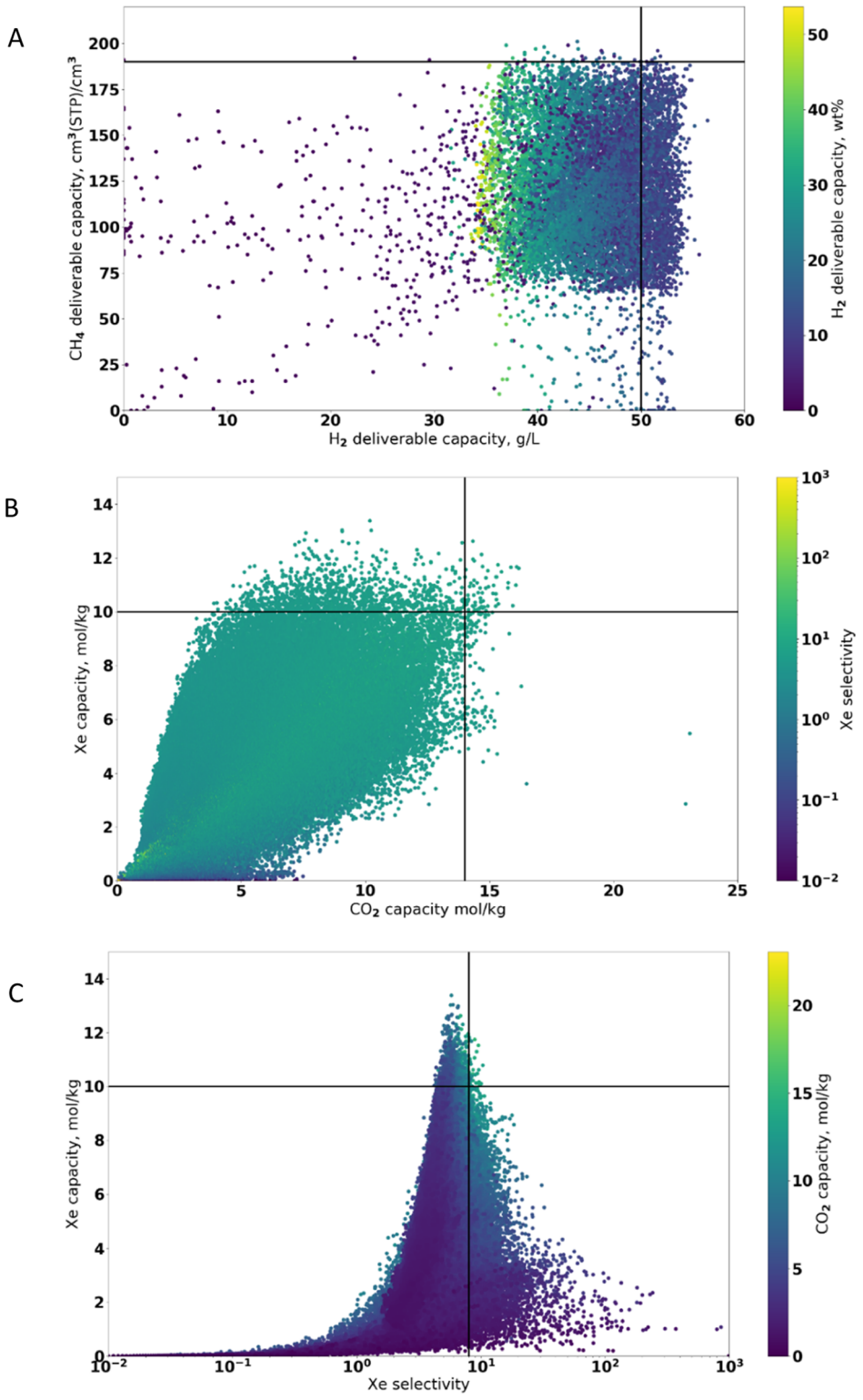

Figure 6. Screening of ToBaCCo MOFs. Conditions are described in the text. (A) Deliverable capacity of methane in $cm^3(STP)/cm^3$ *vs* deliverable capacity of hydrogen in g/L. Each dot represents a single MOF, and the color scale indicates the deliverable capacity of hydrogen in wt %. The vertical and horizontal black lines indicate our criteria for determining the top candidates [50 g/L hydrogen and 190 $cm^3(STP)/cm^3$ methane capacity]. (B) Xe capacity in mol/kg *vs* CO_2 capacity in mol/kg. The color scale indicates the selectivity for Xe over Kr in a binary mixture. The black lines indicate our criteria for determining the top candidates (14 mol/kg CO_2 capacity and 10 mol/kg Xe capacity). (C) Xe capacity in mol/kg *vs* Xe selectivity over Kr in a binary mixture. The color scale indicates the CO_2 capacity, and the black lines indicate the criteria for determining the top MOFs (Xe selectivity greater than 8 and Xe capacity above 10 mol/kg).

specific application (*e.g.*, methane storage or carbon capture), we search the database of published data for MOFs that have good performance for two applications, thereby increasing the utility and commercial attractiveness of that MOF. We offer two examples: MOFs that have high capacity for both hydrogen and methane storage and MOFs with high capacity

https://doi.org/10.1021/acs.jced.2c00583
J. Chem. Eng. Data XXXX, XXX, XXX−XXX

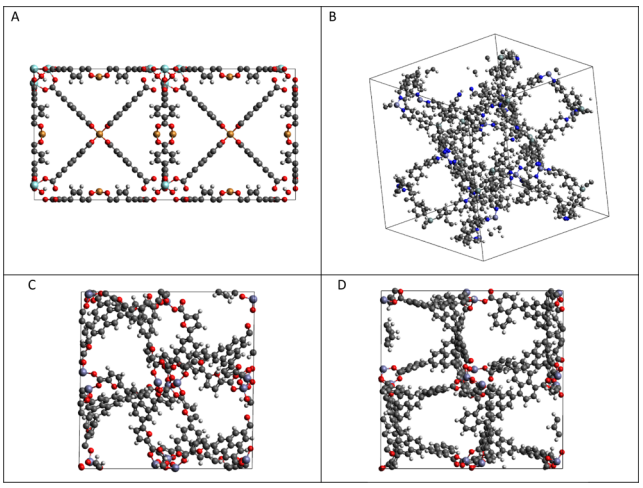

Figure 7. Visualizations of the top four ToBaCCo MOFs for hydrogen and methane storage based on the criteria described in this work. (A) tobmof-3115, (B) tobmof-4253, (C) tobmof-7773, and (D) tobmof-7776. Color key: gray atoms are C, orange atoms are Cu, red atoms are O, dark blue atoms are N, light blue atoms are Zr, purple atoms are Zn, and green-gray atoms are Si.

and selectivity for Xe/Kr separations as well as good capacity for removing CO_2 from natural gas.

4.2.2. Hydrogen and Methane Storage. Methane and hydrogen are viewed as possible energy storage alternatives to gasoline and batteries for automobiles and heavy duty vehicles. Considerable research effort in the last decade has been devoted to finding adsorbent materials that offer high storage density for methane[69,70] or hydrogen.[29,71] Here we search the database of computer-generated ToBaCCo MOFs created by Colón and Gómez-Gualdrón[4] for candidates that provide high capacity for both hydrogen and methane under relevant conditions as prescribed by the Department of Energy.[72,73]

The figures of merit for this study are the deliverable capacity of gas, defined for hydrogen as storage at 100 bar and 77 K with delivery at 5 bar and 160 K and defined for methane as storage at 298 K and 65 bar with delivery at 298 K and 6 bar. The deliverable capacity is the difference in the amount of gas adsorbed between the delivery and storage conditions. Here we focus on volumetric measures of capacity [g/L for hydrogen and $cm^3(STP)/cm^3$ for methane] because volumetric density is typically the greatest challenge for gas storage.[74] The DOE target for hydrogen storage[72] is 50 g/L and 6.5 wt % (based on total system weight), and the target for methane storage[73] is 263 $cm^3(STP)/cm^3$, which we consider highly ambitious, as no material to date has come close to this target.

The results from our screening analysis are shown in Figure 6A. We find 135 candidates that exceed both 45 g/L hydrogen storage and 180 $cm^3(STP)/cm^3$ methane storage. Both of these metrics would be competitive with the highest-performing MOFs reported for each respective application.[50,69,71] Refining our search further, we find four materials that exceed both 50 g/L for hydrogen storage and 190 $cm^3(STP)/cm^3$ for methane storage. Additionally, all four of these MOFs exceed the DOE gravimetric hydrogen target of 6.5 wt %, with the highest being 17.5 wt % (tobmof-3115, Figure 7A). This MOF also has a predicted deliverable hydrogen capacity of 38.5 g/L at 77 K using only a pressure swing from 100 to 5 bar and no temperature swing. Therefore, it could be used for methane storage as well as hydrogen storage at multiple storage conditions. The four top MOFs are shown in Figure 7, and their topological and gas adsorption properties are summarized in Table 3. The data and structure files are also available in the online database. The four MOFs have similar textural properties: they all have void fractions ranging from 0.82 to 0.86 and LCDs ranging from 10.5 to 15.6 Å. This suggests that if we are looking for MOFs with high capacity for both hydrogen and methane storage, we should start by focusing on materials with properties in this range. Additional plots with more textural properties such as surface area and void fraction are shown in Figure S5.

4.2.3. Xe/Kr Separations and Natural Gas Upgrading. Separating CO_2 from methane is of great interest for upgrading natural gas and biogas, which can both contain significant levels of CO_2. Xe and Kr are both valuable gases used in applications such as medical imaging and lighting. They are present in the atmosphere in trace quantities and are typically separated from air *via* energy-intensive cryogenic distillation. Xe/Kr separation is also of interest for nuclear fuel processing. Here, we searched the database of hypothetical MOFs devised by Wilmer *et al.*[3] for candidates with high capacity and selectivity for Xe/Kr separations as well as high capacity for natural gas upgrading using data from Sikora[16] and Wilmer.[42]

Natural gas upgrading and carbon capture are complex, multifaceted problems, so we will not attempt in this example to rigorously consider every aspect of the issue, such as economic cost, MOF stability, and process level considerations. Others have discussed these topics elsewhere.[18,19,75−78] Here the figures of merit we use are absolute CO_2 adsorption in mol/kg at 298 K and 2.5 bar (single-component data),

Table 3. Textural and Adsorption Properties of the Top Four MOFs with Both High Hydrogen and Methane Storage Capacity[a]

						H_2 deliverable capacity				methane deliverable capacity
						[100 bar, 77 K] − [5 bar, 160 K]		[100 bar, 77 K] − [5 bar, 77 K]		[65 bar, 298 K] − [6 bar, 298 K]
MOF	void frac.	SA (m^2/g)	SA (m^2/cm^3)	PLD (Å)	LCD (Å)	(g/L)	(wt %)	(g/L)	(wt %)	[$cm^3(STP)/cm^3$]
tobmof-7773	0.86	4556	2214	8.5	10.5	51.6	8.9	24.9	4.1	196
tobmof-4253	0.84	4971	1942	9.2	12.7	51.9	11.2	37.7	7.8	193
tobmof-3115	0.82	3582	2016	7.3	15.6	51.3	17.5	38.5	12.5	192
tobmof-7776	0.85	4711	2066	9.0	12.5	51.1	10.3	34.3	6.6	191

[a]The deliverable capacity is reported for two sets of conditions for hydrogen: loading at 100 bar and 77 K with delivery at 5 bar and 160 K and loading at 100 bar and 77 K with delivery at 5 bar and 77 K. Methane storage is considered at 298 K with loading at 65 bar and delivery at 6 bar. SA indicates the surface area. PLD indicates the pore limiting diameter, and LCD indicates the largest cavity diameter. Sorted by methane capacity.

https://doi.org/10.1021/acs.jced.2c00583
J. Chem. Eng. Data XXXX, XXX, XXX−XXX

Table 4. Textural and Adsorption Properties of the Top Three MOFs That Meet Our Criteria for High CO_2 Capacity, High Xe Capacity, and High Xe/Kr Selectivity[a]

MOF name	void frac.	SA (m^2/g)	PLD (Å)	LCD (Å)	Xe cap. (mol/kg)	Kr cap. (mol/kg)	Xe select.	CO_2 cap. (mol/kg)
hMOF-056488	0.80	3703	5.25	7.25	10.1	4.2	9.7	14.5
hMOF-36162	0.83	2754	8.25	9.75	10.4	4.9	8.4	14.7
hMOF-5067108	0.85	2842	8.25	9.75	10.1	4.9	8.2	14.6

[a]SA indicates the surface area. PLD indicates the pore limiting diameter, and LCD indicates the largest cavity diameter. Xe and Kr capacity and selectivity are at 10 bar and 273 K under mixture conditions (20/80 Xe/Kr). CO_2 capacity is at 2.5 bar and 298 K under single-component conditions. Sorted by Xe selectivity.

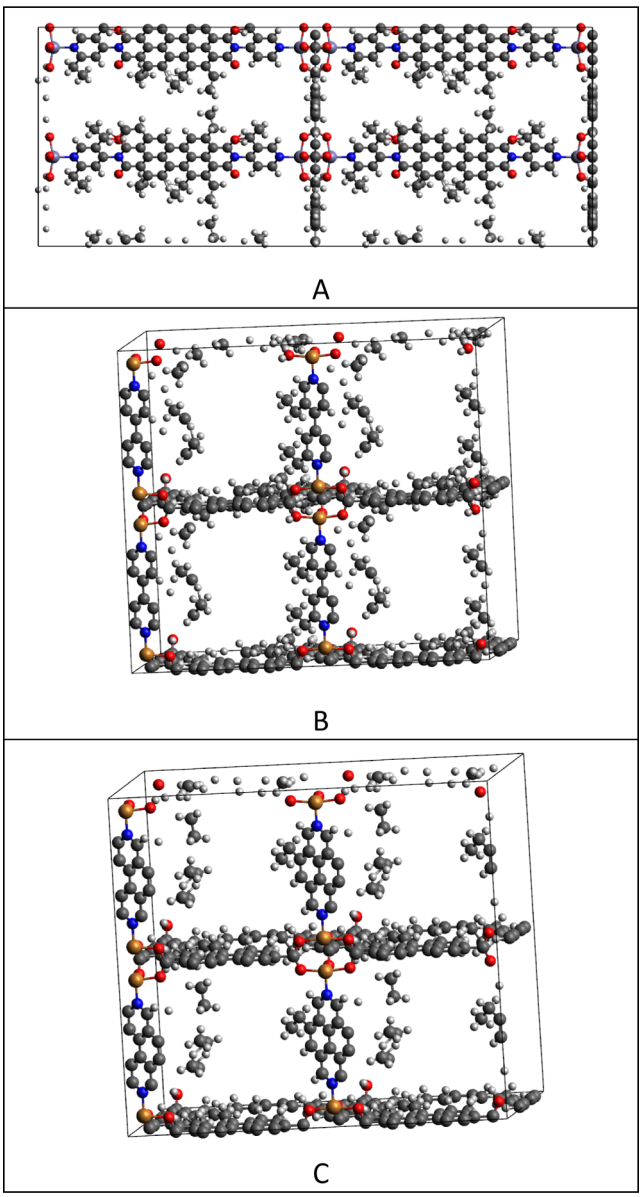

Figure 8. Visualizations of the top three hMOFs for natural gas upgrading and Xe/Kr separation based on the criteria described in this work. (A) hMOF-5056488, (B) hMOF-36162, and (C) hMOF-5067108. Color key: gray atoms are C, orange atoms are Cu, red atoms are O, dark blue atoms are N, and purple atoms are Zn.

absolute Xe adsorption capacity in mol/kg at 10 bar and 273 K (mixture data), and Xe/Kr selectivity at 10 bar and 273 K (mixture data). 2.5 bar is a reasonable pressure for natural gas upgrading,[79,80] so the data from Wilmer's work is relevant.

Xe/Kr simulations were done for a 20/80 mole fraction binary mixture in the adsorptive (gas) phase, and selectivity is computed using $S = (x_{Xe}/y_{Xe})/(x_{Kr}/y_{Kr})$, where x_i represents the adsorbed phase mole fraction and y_i is the gas phase mole fraction. Note that many of the MOFs in this particular database are catenated structures with multiple interpenetrating lattices. Controlling catenation during MOF synthesis is a challenging problem, so in order to avoid complications with the synthesis regarding catenation, we restrict our search to MOFs with only one crystal lattice (no catenation).

Results for this screening are shown in Figure 6B,C. We find 13 MOFs that exceed both 10 mol/kg Xe capacity and 14 mol/kg CO_2 capacity. 14 mol/kg is higher than the capacity of some of the top MOFs reported for CO_2 adsorption, including 8.6 mol/kg in Mg-MOF-74 and 8.4 mol/kg in HKUST-1 at 1 bar,[19] although our data are at a higher pressure of 2.5 bar.

Of these 13 MOFs, 12 have Xe selectivity above 6, which matches the selectivity of the commercial zeolite NaX[81] and is better than NaA, which has a reported selectivity around 4 at 10 atm and 300 K.[82] Three of these structures have Xe selectivity above 8. The textural properties of these three most promising candidates that meet all three criteria (CO_2 capacity above 14 mol/kg, Xe capacity above 10 mol/kg, and Xe selectivity above 8) are shown in Table 4. Visualizations of these three MOFs are shown in Figure 8. All three MOFs have void fractions ranging from 0.80 to 0.85 and LCDs between 7.25 and 9.75 Å. They also have gravimetric surface areas ranging from 2750 to 3700 m^2/g. Notably, the PLDs (5.25 to 8.25 Å) are larger than the kinetic diameter of Kr (3.6 Å), suggesting that the Xe/Kr separation is thermodynamically driven and not based on size exclusion.

5. CONCLUSIONS

In this paper, we present MOFX-DB, a freely available and user-friendly database of simulated adsorption data. MOFX-DB contains adsorption data and textural properties for over 160 000 MOFs and for 286 zeolites, both real and theoretical, as well as all the metadata necessary to reproduce the original simulations, such as GCMC details, force field parameters, and structure files. This database also serves as an archive containing structure files and simulation details that will improve the reproducibility and transparency of research on nanoporous materials. Going forward, we plan to update it regularly with new data. The database also contains (previously unpublished) nitrogen and argon isotherms for CoRE MOFs (including 4764 structures from 2014 version and 12 020 structures from 2019 version), which have all been experimentally synthesized.

The data are presented in an accessible format that is already in use in the NIST-ISODB and has been considered as an informal standard by other groups.[83] We encourage the adsorption community to consider the adoption of this

https://doi.org/10.1021/acs.jced.2c00583
J. Chem. Eng. Data XXXX, XXX, XXX−XXX

JSON isotherm format as a standard for reporting isotherm data in a way that facilitates data exchange between researchers and is conducive to large-scale data mining and machine learning studies in the future.

We have used MOFX-DB here to identify some MOFs that have exceptional performance for multiple applications. We suggest four MOFs with both hydrogen storage capacity above 50 g/L and methane storage capacity exceeding 190 $cm^3(STP)/cm^3$, which are among the best capacities for both gases reported in the literature. We also identify three MOFs with CO_2 capacity above 14 mol/kg and Xe/Kr selectivity above 8, which is better than zeolites NaA and NaX. MOFs such as these that can meet performance targets for multiple applications might be a viable route for encouraging more rapid commercialization of MOFs by broadening markets for a given material and reducing manufacturing costs.

While this paper has been in preparation, a working version of this website has been active for public use. Between January 1, 2020, and July 1, 2022, MOFX-DB has been accessed by over 3500 independent users from 72 countries. Several publications have already been published using data available from this database, which we believe demonstrates its usefulness to the community.[84−87]

Machine learning and data science have made significant contributions to materials science in recent years. We have made this data available to the community in the hopes that it will encourage more studies using data science and yield valuable insights from this data beyond what was included in the original papers.

■ ASSOCIATED CONTENT

Supporting Information

The Supporting Information is available free of charge at https://pubs.acs.org/doi/10.1021/acs.jced.2c00583.

Details about computing textural properties, details of the JSON file format, additional analysis of MOF adsorption data, and information about MOFX-DB version archive (PDF)

■ AUTHOR INFORMATION

Corresponding Author

Randall Q. Snurr − *Department of Chemical and Biological Engineering, Northwestern University, Evanston, Illinois 60208, United States;* orcid.org/0000-0003-2925-9246; Email: snurr@northwestern.edu

Authors

N. Scott Bobbitt − *Department of Chemical and Biological Engineering, Northwestern University, Evanston, Illinois 60208, United States; Material, Physical, and Chemical Sciences Center, Sandia National Laboratories, Albuquerque, New Mexico 87185, United States;* orcid.org/0000-0002-1155-8910

Kaihang Shi − *Department of Chemical and Biological Engineering, Northwestern University, Evanston, Illinois 60208, United States*

Benjamin J. Bucior − *Department of Chemical and Biological Engineering, Northwestern University, Evanston, Illinois 60208, United States;* orcid.org/0000-0002-8545-3898

Haoyuan Chen − *Department of Chemical and Biological Engineering, Northwestern University, Evanston, Illinois 60208, United States; Department of Chemistry, The University of Texas Rio Grande Valley, Edinburg, Texas 78539, United States;* orcid.org/0000-0002-8634-4028

Nathaniel Tracy-Amoroso − *Department of Chemical and Biological Engineering, Northwestern University, Evanston, Illinois 60208, United States*

Zhao Li − *Department of Chemical and Biological Engineering, Northwestern University, Evanston, Illinois 60208, United States;* orcid.org/0000-0001-5035-4614

Yangzesheng Sun − *Department of Chemistry and Chemical Theory Center, University of Minnesota, Minneapolis, Minnesota 55455, United States;* orcid.org/0000-0002-6505-6473

Julia H. Merlin − *School of Chemical and Biomolecular Engineering, Georgia Institute of Technology, Atlanta, Georgia 30332, United States*

J. Ilja Siepmann − *Department of Chemistry and Chemical Theory Center, University of Minnesota, Minneapolis, Minnesota 55455, United States;* orcid.org/0000-0003-2534-4507

Daniel W. Siderius − *Chemical Sciences Division, National Institute of Standards and Technology, Gaithersburg, Maryland 20899, United States;* orcid.org/0000-0002-6260-7727

Complete contact information is available at: https://pubs.acs.org/10.1021/acs.jced.2c00583

Notes

The authors declare no competing financial interest.

■ ACKNOWLEDGMENTS

This research was supported by the U.S. Department of Energy, Office of Basic Energy Sciences, Division of Chemical Sciences, Geosciences and Biosciences under award DE-FG02-17ER16362. The authors thank Thang Pham for assistance with the units conversion function in MOFX-DB. Official contribution of the National Institute of Standards and Technology (NIST), not subject to copyright in the United States of America. Certain commercially available items may be identified in this paper. This identification neither does imply recommendation by NIST nor does it imply that it is the best available for the purposes described. Development of the NIST/ARPA-E Database of Novel and Emerging Adsorbent Materials was funded in part by the Advanced Research Projects Agency-Energy (ARPA-E) through Interagency Agreement Number 1208-0000. Additional computer resources were provided by the Minnesota Supercomputing Institute at the University of Minnesota. H.C. acknowledges the start-up funding from The University of Texas Rio Grande Valley. This work was funded by the Laboratory Directed Research and Development program at Sandia National Laboratories. Sandia National Laboratories is a multimission laboratory managed and operated by National Technology & Engineering Solutions of Sandia, LLC, a wholly owned subsidiary of Honeywell International Inc., for the U.S. Department of Energy's National Nuclear Security Administration under contract DE-NA0003525. This article has been authored by an employee of National Technology & Engineering Solutions of Sandia, LLC under contract no. DE-NA0003525 with the U.S. Department of Energy (DOE). The employee owns all right, title, and interest in and to the article and is solely responsible for its contents. The United States Government retains and the publisher, by accepting the article for

https://doi.org/10.1021/acs.jced.2c00583
J. Chem. Eng. Data XXXX, XXX, XXX−XXX

REFERENCES

(1) Zhou, H. C.; Kitagawa, S. Metal−Organic Frameworks (MOFs). *Chem. Soc. Rev.* **2014**, *43*, 5415−5418.
(2) Chung, Y. G.; Haldoupis, E.; Bucior, B. J.; Haranczyk, M.; Lee, S.; Zhang, H.; Vogiatzis, K. D.; Milisavljevic, M.; Ling, S.; Camp, J. S.; Slater, B.; Siepmann, J. I.; Sholl, D. S.; Snurr, R. Q. Advances, Updates, and Analytics for the Computation-Ready, Experimental Metal−Organic Framework Database: Core MOF 2019. *J. Chem. Eng. Data* **2019**, *64*, 5985−5998.
(3) Wilmer, C. E.; Leaf, M.; Lee, C. Y.; Farha, O. K.; Hauser, B. G.; Hupp, J. T.; Snurr, R. Q. Large-Scale Screening of Hypothetical Metal−Organic Frameworks. *Nat. Chem.* **2012**, *4*, 83.
(4) Colón, Y. J.; Gómez-Gualdrón, D. A.; Snurr, R. Q. Topologically Guided, Automated Construction of Metal−Organic Frameworks and Their Evaluation for Energy-Related Applications. *Cryst. Growth Des.* **2017**, *17*, 5801−5810.
(5) Fernandez, M.; Boyd, P. G.; Daff, T. D.; Aghaji, M. Z.; Woo, T. K. Rapid and Accurate Machine Learning Recognition of High Performing Metal Organic Frameworks for CO_2 Capture. *J. Phys. Chem. Lett.* **2014**, *5*, 3056−3060.
(6) Simon, C. M.; Kim, J.; Gomez-Gualdron, D. A.; Camp, J. S.; Chung, Y. G.; Martin, R. L.; Mercado, R.; Deem, M. W.; Gunter, D.; Haranczyk, M.; Sholl, D. S.; Snurr, R. Q.; Smit, B. The Materials Genome in Action: Identifying the Performance Limits for Methane Storage. *Energy Environ. Sci.* **2015**, *8*, 1190−1199.
(7) Anderson, R.; Gómez-Gualdrón, D. A. Increasing Topological Diversity During Computational "Synthesis" of Porous Crystals: How and Why. *CrystEngComm* **2019**, *21*, 1653−1665.
(8) Colón, Y. J.; Snurr, R. Q. High-Throughput Computational Screening of Metal−Organic Frameworks. *Chem. Soc. Rev.* **2014**, *43*, 5735−5749.
(9) Sturluson, A.; Huynh, M. T.; Kaija, A. R.; Laird, C.; Yoon, S.; Hou, F.; Feng, Z.; Wilmer, C. E.; Colón, Y. J.; Chung, Y. G.; Siderius, D. W.; Simon, C. M. The Role of Molecular Modelling and Simulation in the Discovery and Deployment of Metal-Organic Frameworks for Gas Storage and Separation. *Mol. Simul.* **2019**, *45*, 1082−1121.
(10) Fraux, G.; Chibani, S.; Coudert, F.-X. Modelling of Framework Materials at Multiple Scales: Current Practices and Open Questions. *Philos. Trans. R. Soc., A* **2019**, *377*, 20180220.
(11) Boyd, P.; Lee, Y.; Smit, B. Computational Development of the Nanoporous Materials Genome. *Nat. Rev. Mater.* **2017**, *2*, 17037.
(12) Thornton, A. W.; Simon, C. M.; Kim, J.; Kwon, O.; Deeg, K. S.; Konstas, K.; Pas, S. J.; Hill, M. R.; Winkler, D. A.; Haranczyk, M.; Smit, B. Materials Genome in Action: Identifying the Performance Limits of Physical Hydrogen Storage. *Chem. Mater.* **2017**, *29*, 2844−2854.
(13) Gopalan, A.; Bucior, B. J.; Bobbitt, N. S.; Snurr, R. Q. Prediction of Hydrogen Adsorption in Nanoporous Materials from the Energy Distribution of Adsorption Sites. *Mol. Phys.* **2019**, *117*, 3683−3694.
(14) Watanabe, T.; Sholl, D. S. Accelerating Applications of Metal−Organic Frameworks for Gas Adsorption and Separation by Computational Screening of Materials. *Langmuir* **2012**, *28*, 14114−14128.
(15) Tang, D.; Wu, Y.; Verploegh, R. J.; Sholl, D. S. Efficiently Exploring Adsorption Space to Identify Privileged Adsorbents for Chemical Separations of a Diverse Set of Molecules. *ChemSusChem* **2018**, *11*, 1567−1575.
(16) Sikora, B. J.; Wilmer, C. E.; Greenfield, M. L.; Snurr, R. Q. Thermodynamic Analysis of Xe/Kr Selectivity in over 137000 Hypothetical Metal−Organic Frameworks. *Chem. Sci.* **2012**, *3*, 2217−2223.
(17) Chung, Y. G.; Bai, P.; Haranczyk, M.; Leperi, K. T.; Li, P.; Zhang, H.; Wang, T. C.; Duerinck, T.; You, F.; Hupp, J. T.; Farha, O. K.; Siepmann, J. I.; Snurr, R. Q. Computational Screening of Nanoporous Materials for Hexane and Heptane Isomer Separation. *Chem. Mater.* **2017**, *29*, 6315−6328.
(18) Boyd, P. G.; Chidambaram, A.; García-Díez, E.; Ireland, C. P.; Daff, T. D.; Bounds, R.; Gładysiak, A.; Schouwink, P.; Moosavi, S. M.; Maroto-Valer, M. M. Data-Driven Design of Metal−Organic Frameworks for Wet Flue Gas CO_2 Capture. *Nature* **2019**, *576*, 253−256.
(19) Yu, J.; Xie, L.-H.; Li, J.-R.; Ma, Y.; Seminario, J. M.; Balbuena, P. B. CO_2 Capture and Separations Using MOFs: Computational and Experimental Studies. *Chem. Rev.* **2017**, *117*, 9674−9754.
(20) Chen, H.; Chen, Z.; Zhang, L.; Li, P.; Liu, J.; Redfern, L. R.; Moribe, S.; Cui, Q.; Snurr, R. Q.; Farha, O. K. Toward Design Rules of Metal−Organic Frameworks for Adsorption Cooling: Effect of Topology on the Ethanol Working Capacity. *Chem. Mater.* **2019**, *31*, 2702−2706.
(21) Li, W.; Xia, X.; Cao, M.; Li, S. Structure−Property Relationship of Metal−Organic Frameworks for Alcohol-Based Adsorption-Driven Heat Pumps Via High-Throughput Computational Screening. *J. Mater. Chem. A* **2019**, *7*, 7470−7479.
(22) Erdős, M. t.; de Lange, M. F.; Kapteijn, F.; Moultos, O. A.; Vlugt, T. J. In Silico Screening of Metal−Organic Frameworks for Adsorption-Driven Heat Pumps and Chillers. *ACS Appl. Mater. Interfaces* **2018**, *10*, 27074−27087.
(23) Rosen, A. S.; Notestein, J. M.; Snurr, R. Q. Identifying Promising Metal−Organic Frameworks for Heterogeneous Catalysis Via High-Throughput Periodic Density Functional Theory. *J. Comput. Chem.* **2019**, *40*, 1305−1318.
(24) Ye, J.; Gagliardi, L.; Cramer, C. J.; Truhlar, D. G. Computational Screening of MOF-Supported Transition Metal Catalysts for Activity and Selectivity in Ethylene Dimerization. *J. Catal.* **2018**, *360*, 160−167.
(25) Gustafson, J. A.; Wilmer, C. E. Computational Design of Metal−Organic Framework Arrays for Gas Sensing: Influence of Array Size and Composition on Sensor Performance. *J. Phys. Chem. C* **2017**, *121*, 6033−6038.
(26) Greathouse, J. A.; Ockwig, N. W.; Criscenti, L. J.; Guilinger, T.; Pohl, P.; Allendorf, M. D. Computational Screening of Metal−Organic Frameworks for Large-Molecule Chemical Sensing. *Phys. Chem. Chem. Phys.* **2010**, *12*, 12621−12629.
(27) Fernandez, M.; Woo, T. K.; Wilmer, C. E.; Snurr, R. Q. Large-Scale Quantitative Structure−Property Relationship (QSPR) Analysis of Methane Storage in Metal−Organic Frameworks. *J. Phys. Chem. C* **2013**, *117*, 7681−7689.
(28) Ahmed, A.; Seth, S.; Purewal, J.; Wong-Foy, A. G.; Veenstra, M.; Matzger, A. J.; Siegel, D. J. Exceptional Hydrogen Storage Achieved by Screening Nearly Half a Million Metal-Organic Frameworks. *Nat. Commun.* **2019**, *10*, 1568.
(29) Bobbitt, N. S.; Chen, J.; Snurr, R. Q. High-Throughput Screening of Metal−Organic Frameworks for Hydrogen Storage at Cryogenic Temperature. *J. Phys. Chem. C* **2016**, *120*, 27328−27341.
(30) Bucior, B. J.; Bobbitt, N. S.; Islamoglu, T.; Goswami, S.; Gopalan, A.; Yildirim, T.; Farha, O. K.; Bagheri, N.; Snurr, R. Q. Energy-Based Descriptors to Rapidly Predict Hydrogen Storage in Metal−Organic Frameworks. *Mol. Syst. Des. Eng.* **2019**, *4*, 162−174.
(31) Iacomi, P.; Llewellyn, P. L. Data Mining for Binary Separation Materials in Published Adsorption Isotherms. *Chem. Mater.* **2020**, *32*, 982−991.
(32) Siderius, D. W., Shen, V. K., Johnson, R. D., van Zee, R. D., Eds. *NIST/ARPA-E Database of Novel and Emerging Adsorbent Materials*;

https://doi.org/10.1021/acs.jced.2c00583
J. Chem. Eng. Data XXXX, XXX, XXX−XXX

National Institute of Standards and Technology: Gaithersburg, MD, 20899, 2020.
(33) Chung, Y. G.; Camp, J.; Haranczyk, M.; Sikora, B. J.; Bury, W.; Krungleviciute, V.; Yildirim, T.; Farha, O. K.; Sholl, D. S.; Snurr, R. Q. Computation-Ready, Experimental Metal−Organic Frameworks: A Tool to Enable High-Throughput Screening of Nanoporous Crystals. *Chem. Mater.* **2014**, *26*, 6185−6192.
(34) Moghadam, P. Z.; Li, A.; Wiggin, S. B.; Tao, A.; Maloney, A. G.; Wood, P. A.; Ward, S. C.; Fairen-Jimenez, D. Development of a Cambridge Structural Database Subset: A Collection of Metal−Organic Frameworks for Past, Present, and Future. *Chem. Mater.* **2017**, *29*, 2618−2625.
(35) Vines, T. H.; Albert, A. Y.; Andrew, R. L.; Débarre, F.; Bock, D. G.; Franklin, M. T.; Gilbert, K. J.; Moore, J.-S.; Renaut, S.; Rennison, D. J. The Availability of Research Data Declines Rapidly with Article Age. *Curr. Biol.* **2014**, *24*, 94−97.
(36) Krawczyk, M.; Reuben, E. (Un)Available Upon Request: Field Experiment on Researchers' Willingness to Share Supplementary Materials. *Acc. Res.* **2012**, *19*, 175−186.
(37) Gabelica, M.; Bojčić, R.; Puljak, L. Many Researchers Were Not Compliant with Their Published Data Sharing Statement: Mixed-Methods Study. *J. Clin. Epidemiol.* **2022**, *150*, 33−41.
(38) Moghadam, P. Z.; Islamoglu, T.; Goswami, S.; Exley, J.; Fantham, M.; Kaminski, C. F.; Snurr, R. Q.; Farha, O. K.; Fairen-Jimenez, D. Computer-Aided Discovery of a Metal−Organic Framework with Superior Oxygen Uptake. *Nat. Commun.* **2018**, *9*, 1378.
(39) MilliporeSigma. Digitizing Data: A Report of Current Challenges, *American Chemical Society C&EN White Paper*, 2021.
(40) Coudert, F. X. Materials Databases: The Need for Open, Interoperable Databases with Standardized Data and Rich Metadata. *Adv. Theory Simul.* **2019**, *2*, 1900131.
(41) Wilkinson, M. D.; Dumontier, M.; Aalbersberg, I. J.; Appleton, G.; Axton, M.; Baak, A.; Blomberg, N.; Boiten, J.-W.; da Silva Santos, L. B.; Bourne, P. E.; Bouwman, J. The Fair Guiding Principles for Scientific Data Management and Stewardship. *Sci. Data* **2016**, *3*, 160018.
(42) Wilmer, C. E.; Farha, O. K.; Bae, Y.-S.; Hupp, J. T.; Snurr, R. Q. Structure−Property Relationships of Porous Materials for Carbon Dioxide Separation and Capture. *Energy Environ. Sci.* **2012**, *5*, 9849−9856.
(43) Gómez-Gualdrón, D. A.; Colón, Y. J.; Zhang, X.; Wang, T. C.; Chen, Y.-S.; Hupp, J. T.; Yildirim, T.; Farha, O. K.; Zhang, J.; Snurr, R. Q. Evaluating Topologically Diverse Metal−Organic Frameworks for Cryo-Adsorbed Hydrogen Storage. *Energy Environ. Sci.* **2016**, *9*, 3279−3289.
(44) Chung, Y. G.; Camp, J.; Haranczyk, M.; Sikora, B.; Bury, W.; Krungleviciute, V.; Yildirum, T.; Farha, O. K.; Sholl, D. S.; Snurr, R. Q. Computation-Ready, Experimental Metal−Organic Frameworks. https://zenodo.org/record/3228673 (accessed June 22, 2022).
(45) Chung, Y. G.; Haldoupis, E.; Bucior, B. J.; Haranczyk, M.; Lee, S.; Vogiatzis, K. D.; Ling, S.; Milisavljevic, M.; Zhang, H.; Camp, J. S.; Slater, B.; Seipman, J. I.; Sholl, D. S.; Snurr, R. Q. Computation-Ready Experimental Metal-Organic Framework (Core MOF) 2019 Dataset. https://zenodo.org/record/3370144#.Yp6_MKjMJPZ (accessed June 22, 2022).
(46) Sun, Y.; DeJaco, R. F.; Li, Z.; Tang, D.; Glante, S.; Sholl, D. S.; Colina, C. M.; Snurr, R. Q.; Thommes, M.; Hartmann, M.; Siepmann, J. I. Fingerprinting Diverse Nanoporous Materials for Optimal Hydrogen Storage Conditions Using Meta-Learning. *Sci. Adv.* **2021**, *7*, No. eabg3983.
(47) Dubbeldam, D.; Calero, S.; Ellis, D. E.; Snurr, R. Q. Raspa: Molecular Simulation Software for Adsorption and Diffusion in Flexible Nanoporous Materials. *Mol. Simul.* **2016**, *42*, 81−101.
(48) Bucior, B. J.; Rosen, A. S.; Haranczyk, M.; Yao, Z.; Ziebel, M. E.; Farha, O. K.; Hupp, J. T.; Siepmann, J. I.; Aspuru-Guzik, A.; Snurr, R. Q. Identification Schemes for Metal−Organic Frameworks to Enable Rapid Search and Cheminformatics Analysis. *Cryst. Growth Des.* **2019**, *19*, 6682−6697.
(49) Heller, S. R.; McNaught, A.; Pletnev, I.; Stein, S.; Tchekhovskoi, D. InChI, the IUPAC International Chemical Identifier. *J. Cheminf.* **2015**, *7*, 23.
(50) Bobbitt, N. S.; Snurr, R. Q. Molecular Modelling and Machine Learning for High-Throughput Screening of Metal-Organic Frameworks for Hydrogen Storage. *Mol. Simul.* **2019**, *45*, 1069−1081.
(51) Banerjee, D.; Simon, C. M.; Plonka, A. M.; Motkuri, R. K.; Liu, J.; Chen, X.; Smit, B.; Parise, J. B.; Haranczyk, M.; Thallapally, P. K. Metal−Organic Framework with Optimally Selective Xenon Adsorption and Separation. *Nat. Commun.* **2016**, *7*, 11831.
(52) Banerjee, D.; Zhang, Z.; Plonka, A. M.; Li, J.; Parise, J. B. A Calcium Coordination Framework Having Permanent Porosity and High CO_2/N_2 Selectivity. *Cryst. Growth Des.* **2012**, *12*, 2162−2165.
(53) Fielding, R. T.; Taylor, R. N. *Architectural Styles and the Design of Network-Based Software Architectures*; University of California, Irvine: Irvine, 2000; Vol. 7.
(54) Siderius, D. W.; Shen, V. K. *The NIST Registry of Adsorbent Materials*; National Institute of Standards and Technology: Gaithersburg, MD, 20899, retrieved October 18, 2021.
(55) Evans, J. D.; Bon, V.; Senkovska, I.; Kaskel, S. A Universal Standard Archive File for Adsorption Data. *Langmuir* **2021**, *37*, 4222−4226.
(56) As discussed in the Supporting Information, we refer to the external bulk fluid phase as the "adsorptive phase".
(57) Wu, S.; Ma, L.; Long, L.-S.; Zheng, L.-S.; Lin, W. Three-Dimensional Metal-Organic Frameworks Based on Functionalized Tetracarboxylate Linkers: Synthesis, Strucures, and Gas Sorption Studies. *Inorg. Chem.* **2009**, *48*, 2436−2442.
(58) Wu, S.; Ma, L.; Long, L.-S.; Zheng, L.-S.; Lin, W. *CCDC 727296: Experimental Crystal Structure Determination*, 2009.
(59) Rappé, A. K.; Casewit, C. J.; Colwell, K.; Goddard, W. A., III; Skiff, W. M. UFF, a Full Periodic Table Force Field for Molecular Mechanics and Molecular Dynamics Simulations. *J. Am. Chem. Soc.* **1992**, *114*, 10024−10035.
(60) Potoff, J. J.; Siepmann, J. I. Vapor−Liquid Equilibria of Mixtures Containing Alkanes, Carbon Dioxide, and Nitrogen. *AIChE J.* **2001**, *47*, 1676−1682.
(61) Dinpajooh, M.; Bai, P.; Allan, D. A.; Siepmann, J. I. Accurate and Precise Determination of Critical Properties from Gibbs Ensemble Monte Carlo Simulations. *J. Chem. Phys.* **2015**, *143*, 114113.
(62) Pillai, R. S.; Pinto, M. L.; Pires, J.; Jorge, M.; Gomes, J. R. Understanding Gas Adsorption Selectivity in Irmof-8 Using Molecular Simulation. *ACS Appl. Mater. Interfaces* **2015**, *7*, 624−637.
(63) Li, J.; Yang, J.; Li, L.; Li, J. Separation of CO_2/CH_4 and CH_4/N_2 Mixtures Using MOF-5 and $Cu_3(BTC)_2$. *J. Energy Chem.* **2014**, *23*, 453−460.
(64) Tahmooresi, M.; Sabzi, F. Sorption of Methane in a Series of Zn-Based MOFs Studied by Phsc Equation of State. *Fluid Phase Equilib.* **2014**, *381*, 83−89.
(65) Furukawa, H.; Ko, N.; Go, Y. B.; Aratani, N.; Choi, S. B.; Choi, E.; Yazaydin, A. Ö.; Snurr, R. Q.; O'Keeffe, M.; Kim, J.; Yaghi, O. M. Ultrahigh Porosity in Metal-Organic Frameworks. *Science* **2010**, *329*, 424−428.
(66) Li, H.; Eddaoudi, M.; O'Keeffe, M.; Yaghi, O. M. Design and Synthesis of an Exceptionally Stable and Highly Porous Metal-Organic Framework. *Nature* **1999**, *402*, 276−279.
(67) Eddaoudi, M.; Li, H.; Reineke, T.; Fehr, M.; Kelley, D.; Groy, T. L.; Yaghi, O. Design and Synthesis of Metal-Carboxylate Frameworks with Permanent Microporosity. *Top. Catal.* **1999**, *9*, 105−111.
(68) Eddaoudi, M.; Li, H.; Reineke, T.; Fehr, M.; Kelley, D.; Groy, T. L.; Yaghi, O. M. *CCDC 256965: Experimental Crystal Structure Determination*, 2005.
(69) Dailly, A.; Beckner, M. Methane Storage on Metal-Organic Frameworks. *Nanoporous Materials for Gas Storage*; Springer, 2019; pp 227−253.

https://doi.org/10.1021/acs.jced.2c00583
J. Chem. Eng. Data XXXX, XXX, XXX−XXX

(70) Gómez-Gualdrón, D. A.; Wilmer, C. E.; Farha, O. K.; Hupp, J. T.; Snurr, R. Q. Exploring the Limits of Methane Storage and Delivery in Nanoporous Materials. *J. Phys. Chem. C* **2014**, *118*, 6941−6951.
(71) Allendorf, M. D.; Hulvey, Z.; Gennett, T.; Ahmed, A.; Autrey, T.; Camp, J.; Cho, E. S.; Furukawa, H.; Haranczyk, M.; Head-Gordon, M.; Jeong, S.; Karkamkar, A.; Liu, D.-J.; Long, J. R.; Meihaus, K. R.; Nayyar, I.; Nazarov, R.; Siegel, D. J.; Stavila, V.; Urban, J. J.; Veccham, S. P.; Wood, B. C. An Assessment of Strategies for the Development of Solid-State Adsorbents for Vehicular Hydrogen Storage. *Energy Environ. Sci.* **2018**, *11*, 2784−2812.
(72) US Department of Energy. DOE Technical Targets for Onboard Hydrogen Storage for Light-Duty Vehicles. https://www.energy.gov/eere/fuelcells/doe-technical-targets-onboard-hydrogen-storage-light-duty-vehicles (accessed January 29, 2020).
(73) US Department of Energy. Methane Opportunities in Vehicular Energy (Move). https://arpa-e-foa.energy.gov/ (accessed January 29, 2020).
(74) Gómez-Gualdrón, D. A.; Wang, T. C.; García-Holley, P.; Sawelewa, R. M.; Argueta, E.; Snurr, R. Q.; Hupp, J. T.; Yildirim, T.; Farha, O. K. Understanding Volumetric and Gravimetric Hydrogen Adsorption Trade-Off in Metal−Organic Frameworks. *ACS Appl. Mater. Interfaces* **2017**, *9*, 33419−33428.
(75) Leperi, K. T.; Chung, Y. G.; You, F.; Snurr, R. Q. Development of a General Evaluation Metric for Rapid Screening of Adsorbent Materials for Postcombustion CO_2 Capture. *ACS Sustainable Chem. Eng.* **2019**, *7*, 11529−11539.
(76) Cheng, Y.; Wang, Z.; Zhao, D. Mixed Matrix Membranes for Natural Gas Upgrading: Current Status and Opportunities. *Ind. Eng. Chem. Res.* **2018**, *57*, 4139−4169.
(77) Khan, A.; Qyyum, M. A.; Saulat, H.; Ahmad, R.; Peng, X.; Lee, M. Metal−Organic Frameworks for Biogas Upgrading: Recent Advancements, Challenges, and Future Recommendations. *Appl. Mater. Today* **2021**, *22*, 100925.
(78) Belmabkhout, Y.; Bhatt, P. M.; Adil, K.; Pillai, R. S.; Cadiau, A.; Shkurenko, A.; Maurin, G.; Liu, G.; Koros, W. J.; Eddaoudi, M. Natural Gas Upgrading Using a Fluorinated MOF with Tuned H_2s and CO_2 Adsorption Selectivity. *Nat. Energy* **2018**, *3*, 1059−1066.
(79) Cavenati, S.; Grande, C. A.; Rodrigues, A. E. Separation of $CH_4/CO_2/N_2$ Mixtures by Layered Pressure Swing Adsorption for Upgrade of Natural Gas. *Chem. Eng. Sci.* **2006**, *61*, 3893−3906.
(80) Rallapalli, P. B. S.; Cho, K.; Kim, S. H.; Kim, J.-N.; Yoon, H. C. Upgrading Pipeline-Quality Natural Gas to Liquefied-Quality Via Pressure Swing Adsorption Using Mil-101 (Cr) as Adsorbent to Remove CO_2 and H_2s from the Gas. *Fuel* **2020**, *281*, 118985.
(81) Izumi, J. Waste Gas Treatment Using Zeolites in Nuclear-Related Industries. *Handbook of Zeolite Science and Technology*; CRC Press, 2003; pp 1260−1282.
(82) Jameson, C. J.; Jameson, A. K.; Lim, H.-M. Competitive Adsorption of Xenon and Krypton in Zeolite Naa: 129 Xe Nuclear Magnetic Resonance Studies and Grand Canonical Monte Carlo Simulations. *J. Chem. Phys.* **1997**, *107*, 4364−4372.
(83) Siderius, D. W. Private communication, **2020**.
(84) Lyu, H.; Ji, Z.; Wuttke, S.; Yaghi, O. M. Digital Reticular Chemistry. *Chem* **2020**, *6*, 2219−2241.
(85) Altintas, C.; Altundal, O. F.; Keskin, S.; Yildirim, R. Machine Learning Meets with Metal Organic Frameworks for Gas Storage and Separation. *J. Chem. Inf. Model.* **2021**, *61*, 2131−2146.
(86) Krishnapriyan, A. S.; Montoya, J.; Haranczyk, M.; Hummelshøj, J.; Morozov, D. Machine Learning with Persistent Homology and Chemical Word Embeddings Improves Prediction Accuracy and Interpretability in Metal-Organic Frameworks. *Sci. Rep.* **2021**, *11*, 8888.
(87) Yuyama, S.; Kaneko, H. Correlation between the Metal and Organic Components, Structure Property, and Gas-Adsorption Capacity of Metal−Organic Frameworks. *J. Chem. Inf. Model.* **2021**, *61*, 5785−5792.

https://doi.org/10.1021/acs.jced.2c00583
J. Chem. Eng. Data XXXX, XXX, XXX−XXX